Journal of Aerospace Technology and Management

REFERÊNCIA

CAS, Pedro Luiz Kaled Da et al. An Optimized Hybrid Rocket Motor for the SARA Platform Reentry System. **Journal of Aerospace Technology and Management**, São José dos Campos, v. 4, n. 3, p. 317-330, jul./set. 2012. DOI: https://doi.org/10.5028/jatm.2012.04032312. Disponível em: http://www.scielo.br/scielo.php?script=sci_arttext&pid=S2175-91462012000300317&lng=en&nrm=iso. Acesso em: 04 dez. 2020.

doi: 10.5028/jatm.2012.04032312

An Optimized Hybrid Rocket Motor for the SARA Platform Reentry System

Pedro Luiz Kaled Da Cás, Cristiano Queiroz Vilanova, Manuel Nascimento Dias Barcelos Jr.*, Carlos Alberto Gurgel Veras
Universidade de Brasília - Brasília/DF – Brazil

Abstract: *This paper has described a system design process, based on a multidisciplinary optimization technique, of a conceptual optimized hybrid propellant rocket motor. The proposed engine could be a technological option for the reentry maneuvering system of the Brazilian recoverable satellite (SARA), which was designed by the Brazilian Institute of Aeronautics and Space. The resulting optimized propulsion system must be viewed as a proof of concept allowing comparison to more conventional technologies, i.e., liquid and solid motors. Design effort was conducted for hybrid propellants engines based on a liquefying fuel (solid paraffin) and two different oxidizers, H_2O_2 (90% high-test peroxide) and self-pressurizing N_2O. The multidisciplinary configuration optimization technique was supported on geometrical operating parameters of the motor, rather than on performance, in order to facilitate subsequent design and fabrication. Results from the code presented a hybrid motor, which was considered a competitive alternative for the deboost engine when compared to the traditional chemical systems, solid and liquid bipropellant, and monopropellant. The estimated mass of the reentry system, for the cases addressed in this study, varied from 22 to 29 kg, which is lower than either liquid bipropellant or solid engines formerly proposed.*

Keywords: *Hybrid rocket propulsion, Multiphysics analysis, Design optimization.*

INTRODUCTION

The SARA satellite was conceived as a microgravity recoverable and reusable research platform by both Brazilian Institute of Aeronautics and Space (IAE) and Space Agency (AEB). Figure 1a shows an artistic design of the platform and Fig. 1b, the planned launch vehicle of the spacecraft. The satellite was designed to carry a 55 kg payload mass, with total launch mass not exceeding 350 kg. Missions were projected to take place in circular orbits at 300 km altitude, with two-degree inclination. After completion of the microgravity experiments, up to ten days, the reentry procedure began by providing the right positioning of the satellite followed by the deboost impulse. Final deceleration took place by a high performance parachute system (Koldaev and Moraes, 1997). The spacecraft was scheduled to pass through a series of qualification tests in ballistic flights reaching 350 km apogee and falling at about 300 km from the launch site. The system should be accelerated by a Brazilian VS-40 sounding rocket (Fig. 1b).

To date, solid and liquid rocket propulsion systems were the only technological means considered for the deboost

(a) (b)

Figure 1. The SARA platform atmospheric reentry. (a) artist's impression; (b) the VS-40 rocket. Source: Brazilian Institute of Aeronautics and Space.

Received: 18/04/12 Accepted: 21/06/12
*author for correspondence: manuelbarcelos@gmail.com
Faculdade UnB-Gama- Área Especial 2, Lote 14, Setor Central Gama-DF/ CEP: 72405-610- Brazil

motor (Villas Bôas *et al.*, 2006). Hybrid propellant rocket engines, however, could be a competitive alternative for the reentry system in light of the recent reported technological advances, largely to those concerned with improvements in solid fuel regression rate.

The Universidade de Brasília hybrid propulsion team (HPT - UnB) has a considerable history in developing and testing hybrid rocket engines and small sounding rockets, in which the thrust and burning times (impulse) are quite similar to those claimed by the SARA deboost system (Viegas and Salemi, 2000; Santos, 2006; Contaifer, 2006). Hybrid rockets should be considered an attractive option for the Brazilian space program by virtue of their relative lower development cost, simple construction, and safe operation. This paper thus has described a system design process, based on a multidisciplinary optimization technique, of a conceptual hybrid rocket motor for the reentry maneuver system of the Brazilian recoverable platform (SARA). The resulting optimized propulsion system should be viewed as a proof of concept, allowing direct comparison to the well-known solid and liquid technologies, which were previously investigated by Villas Bôas *et al.* (2006). The optimization code based on a genetic algorithm, as presented in this work, should be considered a modern and essential design assistance tool for a broad utilization of hybrid propellant rocket engines.

HYBRID PROPELLANT ROCKET ENGINES

In spite of all claimed advantages of hybrid rocket engines over the solid and liquid counterparts, the related weaknesses should be analyzed in more details as to assure the technology would not be disregarded following a first assessment for the proposed application (debooster).

Recently, Karabeyoglu (2008) highlighted some nontechnical challenges that hybrid rockets face in the present days: lack of technological maturity; competition against established solid and liquid technologies; propulsion industry fineness with the *status quo*; and smaller groups of rocket professionals regarding solid and liquid rockets.

We add to those nontechnical challenges some key technological disadvantages of hybrid propulsion, compared to solid and liquid corresponding systems as pointed by Altman and Holzman (2007): low regression rate of the solid fuel surface; low bulk density; combustion efficiency; O/F shift; and slower transients.

In a more recent study, Oiknine (2006) analyzed whether the renewal interest of hybrid fuels could lead to a successful commercial venture in the near future. The author claimed that, for a commercial project, the risk of introducing a new low-cost technology should be justified only if the present costs pose relevant financial difficulties. The author also pointed that, when high-thrust level is required, a high fuel mass flow should be delivered, which is, in particular, the primary challenge in hybrid motor operation. This challenge may thus explain the currently observed commercial failure of the hybrid propellant rocket technology.

Davydenko *et al.* (2007) listed key advantages of hybrid propulsion system over either solid, monopropellant or bipropellant propulsions, which, when brought to the desired application, would increase the chances of the anticipated propulsion system, based on:

- safety (in manufacturing, transporting, and storing as a consequence of separate fuel and oxidizer);
- reliability (due to the larger margin of tolerance in grain imperfections as well as ambient conditions);
- flexibility (by virtue of stop-restart capabilities and thrust modulation);
- costs (due to low investments costs for development and operation as well as those costs associated with the materials to fabricate the motor, and general availability of the required materials and technologies);
- environment (since combustion products are often nontoxic gases and propellants are not hazardous to storage and transport).

Compared to liquid rocket engines, Davydenko *et al.* (2007) added that the use of hybrid rocket technology, as suggested in this study, would increase system reliability on account of reduction in:

- propulsion system development periods, from about four years to less than ten months;
- fabrication cost, by a factor of about two, owing to the application of thermal protective carbon-containing composite materials;
- operating costs, by 40 to 50%;
- cost of fire-and-explosion safety systems.

The required thrust level for the SARA reentry system is far less than that for a small launch vehicle, therefore solid regression rate can be considered secondary in performance characteristics. The main disadvantages, listed by Altman and Holzman (2007), seem also not so imperative to

disregard hybrid rocket for the deboost system. Brazil still lacks an established rocket propulsion industry; therefore, introducing a new low-cost technology brings no risk, in contrast, it should be encouraged. The thrust level and burning times of the deboost system do not require high fuel mass flow rate, which may be possible with a single port configuration design, further simplifying the propulsive system. As for the nontechnical challenges, after the paper written by Karabeyoglu (2008), we also believe they are not impeditive to place hybrid propulsion as an essential option for near future consideration of the Brazilian space market. The points raised in Davydenko *et al.* (2007) are also very promising to disregard the hybrid system technology as proposed in this study.

MULTIDISCIPLINARY DESIGN OPTIMIZATION CODING

Genetic algorithm (GA) may be defined as a stochastic search and optimization method with embedded characteristics closely following the biological evolution observed in nature. By such means, the method chose the fittest individuals from generation to generation approaching, successively, a better solution for the problem. GA has been employed, more intensively, in aerospace systems designed after the 1980s (Anderson, 2002). Anderson (2002) has highlighted that the method can be applied to solve aerospace problems in particular fields, such as: guidance, navigation and control; aerodynamics; multidisciplinary design; propulsion; structures; scheduling and control; flight test data extraction, among others. GA can be applied in the conceptual phase of design as a substitute to more traditional trial and error methods. As pointed by Akhtar and Lin-sh (2007), GA, compared to gradient-based methods, allows optimization-like tools to support the conceptual phase of design by combining discrete, integer, and continuous variables with no requirement for an initial design. The method has also the ability to address nonconvex, multimodal, and discontinuous functions of a given problem (Akhtar and Lin-sh, 2007). More recently, optimization analysis of hybrid rocket engines has been applied to launch vehicles (Rhee *et al.*, 2008; DaLin *et al.*, 2012).

An optimization problem can be expressed as the minimization of an objective function under certain equality and inequality constraints. The formulation of a generic optimization problem is defined as Eqs. 1 to 4:

$$\min_{s \in S} z(s, q(s)) \quad (1)$$

$$h(s, q(s)) = 0, h \in R^{\eta_h} \quad (2)$$

$$g(s, q(s)) < 0, g \in R^{\eta g} \quad (3)$$

$$S = \{s \in R^{\eta s} \mid S_L \leq S \leq S_U\} \quad (4)$$

where,
z is the objective function,
s is the set of design variables,
q is the set of design criteria, and
h and g are respectively equality and inequality constraints.

The design variables and constraints belong to a set of real numbers, whose dimensions are represented by n_s, n_h and n_g, respectively. The values of the design variables are limited by lower and upper bounds ($[S_L, S_U]$), defining the so-called box constraints.

The objective function and the constraints are built as functions of design criteria and design variables. In a multidisciplinary design optimization setup, the design variables are defined by parameters that represent different physical aspects. For instance, in hybrid propulsion systems, parameters, such as geometry or shape, dimensions and pressure of the combustion chamber and the mass flow rate of oxidant, may be taken as design variables.

In a multidisciplinary optimization framework, the design criteria are associated with quantities that describe system performance and behavior. As regarded to hybrid propulsion systems, quantities such as trust, burning time, variation of velocity and mass may be considered as design criteria. In general, for a multidisciplinary optimization problem, the design criteria are dependent on the response of the multidisciplinary system, which can also be a function of the design variables.

PROBLEM STATEMENT AND METHODS

A candidate hybrid rocket engine to perform the reentry mission would be composed, basically, of a convergent-divergent nozzle, a combustion chamber, a liquid oxidizer tank, and a gas pressurization subsystem. The latter would be disregarded, depending on the choice of the oxidizer. For instance, the self-pressurizing characteristics of nitrous oxide would circumvent the use of such subsystem.

In its final design, the shape and positioning of the tanks should take the room availability in the engine bay of the SARA spacecraft into account (Fig. 2). Figure 3 shows the proposed reentry motor configurations. The first hybrid

engine relies on a self-pressurizing N_2O and paraffin-based solid fuel (Almeida and Santos, 2005). A pressurizing subsystem is therefore not necessary, simplifying the final design complexity and cost for the reentry motor. The SARA spacecraft was also conceived to have an attitude control system. If nitrous oxide is the preferred oxidizer, the system could be based both on cold gas or thermo catalytic decomposition of N_2O, unifying all the spacecraft propulsive requirements accordingly (Campbell *et al.*, 2008).

The second proposition is more conventional, as it is based on hydrogen peroxide and on a pressurization subsystem. In both cases, paraffin was considered as the solid fuel. An injector plate based on pressure swirl atomizers was chosen for oxidizer injection into the combustion chamber. This system would significantly increase the solid fuel regression rate as compared to a showerhead injector type. The hybrid motor would be made of a cylindrical container with spherical ends. The nozzle would be of conic shape, made of aluminum with carbon phenolic insert for thermal protection. The combustion chamber should also be made of aluminum with added thermal insulation for the postcombustion chamber.

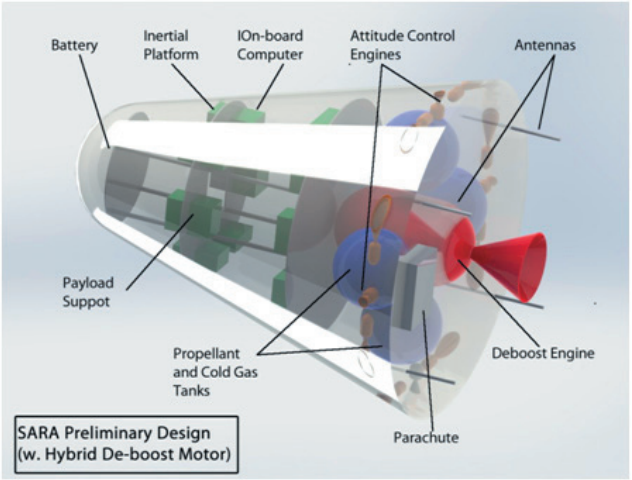

Figure 2. Conceptual design of the SARA platform (with hybrid deboost motor), which was based on a concept by the Brazilian Institute of Aeronautics and Space with the main subsystems.

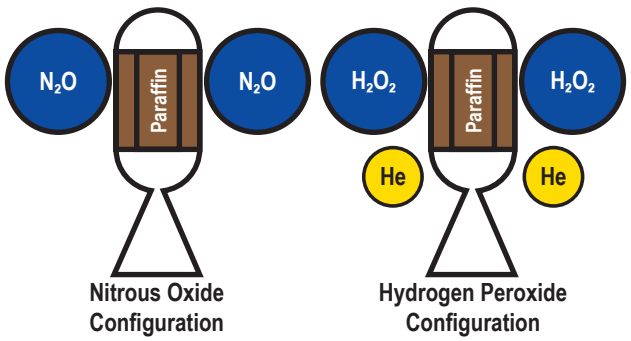

Figure 3. Processes diagram, ModeFRONTIER coding.

The main reentry mission aspects were presented and discussed by Villas Bôas *et al.* (2000), namely: deboost impulse should produce a velocity reduction of the order of 235 to 250 m/s; and total burning time of the motor should be between 50 and 200 seconds.

These performance characteristics, though, are not standalone. The propulsive system should also be subjected to geometric constraints, as well as total mass limitation, on account of the launch vehicle operational envelope and overall mission efficiency. Following that, Villas Bôas *et al.* (2000) proposed three different configurations for the engine (debooster): liquid bipropellant (LBP), liquid monopropellant (LMP), and solid propellant (SP). The LBP alternative was composed of a liquid rocket engine system based on unsymmetrical dimethylhydrazine (UDMH) and nitrogen tetroxide (NTO), with engine chamber feeding provided by means of an inert gas (nitrogen) pressurization subsystem. The second option (LMP) was a hydrazine monopropellant system. As for the LBP, engine chamber feeding should also be provided by an inert gas (nitrogen) pressurization subsystem. The last configuration (SP) should be based on the technology developed at the IAE for the Roll Control System (PCR/S-IV) of the sounding rocket Sonda-IV. Engine thrust would come from the solid propellant end-burn grain type. The propellant grain was conceived as a variable burning area; final thrust was about five to six times lower than the initial thrust.

Figure 2 shows a conceptual design of the spacecraft and its main components. As it can be seen, the engine for deboosting must meet some dimensional requirements. The study conducted by Villas Bôas *et al.* (2000) showed propulsion system mass varying from 35.1 to 47.3 kg. Size and volume of the systems were not presented, however engine system and subsystem were assumed to fit the engine bay of the SARA platform.

As pointed by Kwon *et al.* (2003), in designing a hybrid motor the grain configuration, combustion efficiency, oxidizer tank pressure, and nozzle configuration are key elements of the engine performance. Geometrical configuration is also a major concern. In their paper, the authors selected the number of ports, the initial oxidizer flux, the combustion chamber pressure, the nozzle expansion ratio, and average *OF* ratio as initial candidate design variables. They performed a preliminary sensitivity analysis to identify the dependence of some candidate design variables to the design constraints and objectives, namely: rocket length, diameter, total mass, and nozzle exit diameter. The authors concluded that the number of ports has a significant influence on the rocket length and

diameter. Additionally, their sensitivity analyses for multiport hybrid engines showed the following:

- initial oxidizer flux could dominantly affect the length and diameter of rocket simultaneously;
- nozzle exit diameter was mainly affected by the combustion chamber pressure and nozzle expansion ratio;
- the average ratio had a small influence on the response parameters like rocket length and diameter, and nozzle exit diameter.

Design variables were selected in order to keep the inherent simplicity of hybrid propulsion systems. Liquefying-based fuels (increased solid regression rate) would anticipate the use of only one combustion port, simplifying grain configuration. To some extent, it was avoided the use as a fundamental design constraint of design criteria, whose dependence on the design variables was not explicitly known such as specific impulse. These parameters, though, were considered along the optimization process. Two different minimum chamber pressures were investigated, as to infer how rocket performance would be a key element on the final design. Based on that and also after running some preliminary cases, the chosen design variables, along with their range, were:

- solid fuel external diameter (m) – $0.05 \leq Df \leq 0.2$;
- solid fuel length (m) – $0.05 \leq L_g \leq 0.5$;
- internal port diameter (m) – $0.025 \leq Di \leq 0.2$;
- initial combustion chamber pressures (MPa) – case 1, $1.0 \leq p_{ci} \leq 5.0$; case 2, $3.0 \leq p_{ci} \leq 5.0$; and
- initial oxidizer mass flow rate (kg/s) – $0.05 \leq \dot{m}_{oxi,0} \leq 2.0$.

The solid fuel external diameter was chosen as a main design variable, due to its intrinsic relation with the volume of the combustion chamber. In order to evaluate a broad range of configurations, the grain external diameter was set to vary from 0.05 to 0.2 m, which is much lower than the diameter of the VS-40 sounding rocket (~1.0 m). This wide range in diameter was selected to allow a high degree of freedom, since computational cost was a minor concern. Grain length was also selected as a major design variable due to its direct influence on mixture ratio and size constraint of the system. The grain initial port diameter or thickness is a measure of the available burning radius, or burning time depending on the average oxidizer mass flux. A constraint was imposed to the initial port diameter as to avoid erosive burn. Accordingly, initial oxidizer mass flux should not exceed 400 kg/(m²s) for standard flow conditions (Greatrix, 2009). The initial chamber pressure influences the thrust of the motor, the thickness of the combustion chamber wall, the oxidizer tank pressure and its wall thickness. The chamber pressure was set to vary from 10 to 50 bars. The very low minimum pressure implies lower weight of structural materials for tanks and the motor itself. Therefore, a penalty in the rocket specific impulse is expected. In contrast, the overall mass of the propulsive system and its performance should present an optimum for a given mission, following the optimization process, which would help clarifying this statement.

A routine with the ESTECO's ModeFRONTIER software (ModeFRONTIERv4) was used to help generate, evaluate, and select individuals along the optimization process. The ModeFRONTIER workflow showed in Fig. 4 consists of a performance prediction module (ballistic model), a set of input variables, and a block with three "IF" structures for the design constraints evaluator, one "IF" node, a GA scheduler, responsible for controlling the GA work, and a design of experiments (DOE) block responsible for controlling the individuals being generated and tested. The performance prediction module was implemented in the MATLAB R2010a Engineering Equation Solver (EES Academic Professional V8-3D). This module has the internal ballistic model proposed in this work. The five input variables block represent the respective design variables described previously. The two design constraint nodes represent the time and velocity variation constraints, $50 < t < 200$ and $Delta\text{-}V > 235$, respectively. The IF node intents at eliminating individuals that fall outside the limitations imposed by the ballistic model. Two limitations were evaluated $D > D_i$ and $4 < OF < 11$, where D was the instantaneous port diameter at any given time.

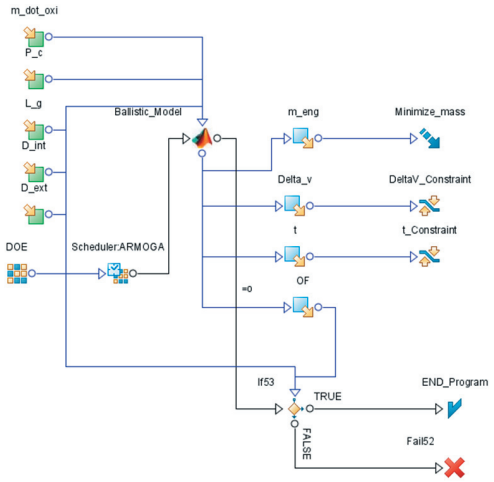

Figure 4. Motor configurations: H_2O_2/paraffin and N_2O/paraffin.

The chosen GA for this optimization was the Adaptive Range Multi-Objective GA (ARMOGA) (Sasaki and Obayashi, 2005). This is a type of GA designed for rapid conversion or Pareto Front formation. It employs variable and adaptive range methodologies that in predetermined periods reevaluate the variable boundaries excluding zones that yielded poor results (Fig. 5). The ARMOGA uses the classic GA parameters, such as mutation, crossover and number of generations, and also the ones for the range adaptation process. The values of these parameters were selected based on several tests and are presented on Table 1. These parameters resulted in the evaluation of 2,519 individuals over the course of 120 generations, although in many of the runs convergence of the majority of the design variables was achieved earlier.

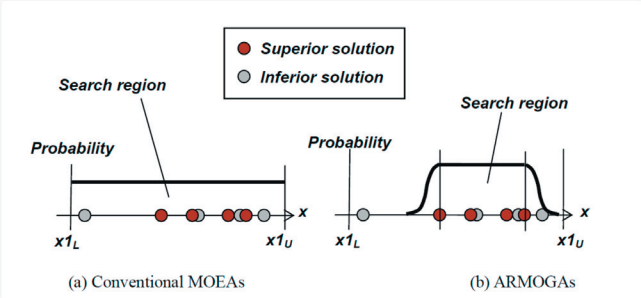

Figure 5. Overview of range adaptation (design range) employed by the ARMOGA algorithm (Sasaki and Obayashi, 2005).

Table 1. Initial setting of the ARMOGA algorithm.

Parameter	Value
Number of generations	120
Star generation of range adaptation	20
Interval generation of range adaptation	20
Probability of crossover	0.9
Probability of mutation	0.1
Ratio of outer region in range adaptation	0.4
Cross over type	Blended
Parameter of crossover	0.5
Mutation type	Polynomial
Parameter of mutation	5.0
Random generator seed	1

INTERNAL BALLISTICS AND ENGINEERING MODELS

The ballistic model for the hybrid motor optimization process has its roots on that proposed by Casalino and Pastrone (2005). The main parameters are shown in Fig. 6.

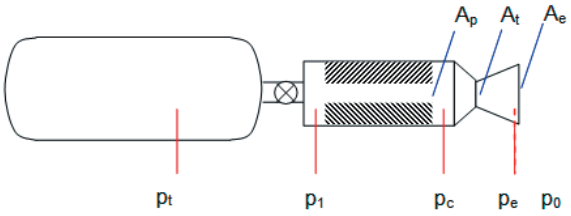

Figure 6. Pressure locations and areas for the ballistic model.

The design of the hybrid rocket engine follows the definition of the initial thrust level, mixture ratio, oxidizer tank pressure, nozzle expansion ratio and the one of throat area to initial port area. Since port area changes as the solid fuel regresses, most of these parameters change during engine operation. The code thus integrates the necessary equations to evaluate the performance of the deboost system along the mission.

Solid fuel regression rate, as a function of the oxidizer mass flux, is calculated through the relation in Eq. 5:

$$\dot{r} = aG_{oxi}^{n}. \tag{5}$$

Values of a and n parameters, appearing in Eq. 1, as proposed by our research group (Bertoldi, 2007) and those of Karabeyoglu *et al.* (2004) can be seen in Table 2, for nitrous oxide and paraffin. The higher regression rate obtained by (Bertoldi, 2007) compared to the latter may be explained by the use of pressure swirl atomizers. For hydrogen peroxide and paraffin, as the propellants, we took regression parameters found in Brown and Lydon (2005).

Table 2. Values of a and n, for G in kg/(m^{2}s) and $\dot{r}$ in mm/s.

Propellants	a	n	Reference
N_2O/paraffin	0.722	0.67	Bertoldi (2007)
N_2O/paraffin	0.488	0.62	Karabeyoglu *et al.* (2004)
H_2O_2/paraffin	0.034	0.96	Brown and Lydon (2005)

Due to the high paraffin regression rate compared to other traditional solid fuels for hybrid propulsion systems, only one combustion port is needed. Therefore, the variation of the internal grain diameter (R) *versus* time is given by Eq. 6:

$$dR/dt = \dot{r}. \tag{6}$$

For pressure variation inside the combustion chamber, we used the following relation in Eq. 7:

$$p_1 = [1 + 0.2(A_t/A_p)^2]p_c. \quad (7)$$

In Eq. 7, p_1 is the head end pressure (oxidizer injection plate) and p_c the combustion chamber pressure just before the expansion process (afterburner). Also, A_t and A_p refer to the area of the throat and grain port, respectively. Oxidizer mass flow rate is a function of the pressure difference through the injection plate, and its hydraulic resistance (Z_{inj}) can be estimated by Eq. 8:

$$\dot{m}_{oxi} = \sqrt{(p_t - p_1)/Z_{inj}} \quad (8)$$

where,

p_t is the oxidizer tank pressure.

The fuel mass flow rate can be calculated by Eq. 9:

$$\dot{m}_f = \rho_f \dot{r} A_b. \quad (9)$$

The fuel mass flow rate in Eq. 9 is a function of the paraffin density (ρ_f), regression rate, and internal burning area of the combustion port (A_b), respectively. The ratio between $\dot{m}_{oxi}$ and provides the mixture ratio of oxidizer and fuel, according to Eq. 10:

$$OF = \dot{m}_{oxi}/\dot{m}_f. \quad (10)$$

The throat area, assuming isentropic expansion, as a function of the chamber pressure in the afterburner section is determined with the help of Eq. 11:

$$A_t = (\dot{m}_{oxi} + \dot{m}_f)c^*/p_c. \quad (11)$$

In Eq. 11, the characteristic velocity was calculated through Eq. 12:

$$c^* = \frac{\sqrt{\gamma R_g T_c}/Y}{\sqrt{\left[\frac{2}{(y+1)}\right]^{\frac{(y+1)}{(y+1)}}}}. \quad (12)$$

The products of combustion and relevant thermodynamic properties were estimated assuming chemical equilibrium. The main parameters were obtained after running the rocket propulsion analysis (RPA) code (Ponomarenko, 2010). Chemical equilibrium was applied for the chosen pair of propellants N_2O/paraffin and H_2O_2/paraffin systems for different ratio and pressure levels. The sensitivity of the reactant products to pressure was considered somehow weak and a mean pressure of 25 bars was chosen for all cases. The data were interpolated accordingly given three polynomials to represent the combustion chamber temperature, $T_c(OF)$; the average molar mass of the combustion products; $MW_c(OF)$ and the specific heat ratio, $\gamma(OF)$ as a function of the mixture ratio for the propellants combination of interest. These polynomials allow an estimation of the thrust coefficient by Eq. 13:

$$C_F = \sqrt{\frac{2y^2}{y-1}\left(\frac{2}{y+1}\right)^{\frac{y-1}{y+1}}\left[1-\left(\frac{Pe}{Pc}\right)^{\frac{y-1}{y}}\right]} + \in\left(\frac{P_e}{P_C} - \frac{P_0}{P_C}\right). \quad (13)$$

The parameters needed to infer the thrust coefficient are: specific heat ratio (γ), nozzle exhaust plane pressure (p_e), ambient pressure (p_0), and nozzle expansion ratio (ε).

The initial geometry of the engine was obtained after inferring the initial mass flow rate of combustion products and initial thrust (F_i) along with the calculated characteristic velocity and thrust coefficient through Eq. 14:

$$\dot{m}_{t,i} = (\dot{m}_f + \dot{m}_{oxi})_i = \frac{F_i}{(c^* C_F)} \quad (14)$$

The throat area was then calculated by Eq. 15:

$$A_t = \dot{m}_{t,i}/(p_{c,i}c^*). \quad (15)$$

The throat area was assumed constant during rocket mission. The initial port area was estimated geometrically (Eq. 16):

$$J_i = A_t/A_{p,i}. \quad (16)$$

This parameter relates the throat area to the initial port one ($A_{p,i} = \pi \cdot D_i^2/4$) of the solid fuel as mean to envelope the oxidizer mass flux. The exit area was calculated for ambient pressure of 0.05 bar and for a mean value of γ. Then, a fixed value of ε was set. The maximum allowed value for ε was 30.

From the initial burning area, it was possible to infer the length of the solid fuel grain, thus characterizing the whole engine.

The instantaneous thrust of the motor can be inferred using mass flow rate as in Eq. 17:

$$F = c^* C_F(\dot{m}_f + \dot{m}_{oxi}). \quad (17)$$

The complete burn time can be estimated by knowing the instantaneous regression rate, the initial port radius, and the final port radius with the help of Eq. 18:

$$t = \int_{R_i}^{R_f} \frac{1}{\dot{r}} dR. \quad (18)$$

The planned velocity variation of the spacecraft, however, should be completed before the system reaches the limit state, as a way to avoid compromising the mission. The desired velocity variation is obtained by integrating the thrust/mass over time (Eq. 19):

$$\Delta V = \int_{t_i}^{t} \frac{F}{m} dt. \quad (19)$$

Once defined the initial engine geometry, the mission performance is evaluated after integrating the relevant equations. The provided spacecraft velocity reduction is compared to the mission requirement, to assert the feasibility of that individual.

The estimated mass of any given individual (engine) is obtained after summing the mass of the combustion chamber, nozzle, oxidizer tanks, pressurization tank, and solid fuel mass. The mass of valves, ignition system, plumbing and other auxiliary devices were not taking into account in the mass model. The contribution of these components should be added to the total mass estimations after the optimization process. Hence, we considered a 20% addition of the optimized engine candidate mass arguing that the mass of the subsystems (catalytic bead for and other components for the ignition system, plumbing, valves etc) is proportional to the mass of the system. This figure is twice as much of that proposed by Costa and Vieira (2010) on account of the lack of reliable data of the components of the propulsive system. All the tanks and combustion chamber would be made of aluminum reinforced with carbon fiber. Mean properties of such composite materials were employed in the mass model. The tanks of oxidant, pressurization subsystem, and structure of the combustion chamber were designed using composite material, aluminum reinforced with carbon, with overall density of 1.8 kg/m^3 and tensile strength limit of 93 MPa. These structural materials were chosen to allow production following the current technological domain of the Brazilian space industry.

Both the oxidizer and pressurizing tanks were spherical, and they were considered as thin walled pressure vessels. The mass of a spherical pressure vessel is given by the Eq. 20:

$$M_{v,1} = \frac{3}{2} p_v V_v \frac{\rho}{\sigma}. \quad (20)$$

where,

ρ and σ are the specific mass and the yielding tension of the tank's material,

p_v and V_v are the design pressure and volume of the stored fluid (vessel).

The code adds a 10% volume for the estimated value of this parameter to accommodate changes in the specific volume due to temperature variations.

The combustion chamber is a cylindrical pressure vessel with spherical ends, in which the mass is estimated by Eq. 21:

$$M_{v,2} = 2\pi R_v^2 (L_v - R_v) p_v \frac{\rho}{\sigma} \quad (21)$$

where,

R_v is the radius of the vessel and L_v its length. The internal diameter of the combustion chamber is equal to the grain external diameter and the vessel's length should accommodate the solid fuel and the postcombustion chamber (10% the solid fuel length). The spherical ends of the chamber account for the masses of the pre and postcombustion chambers and the convergent part of the nozzle.

The nozzle is modeled as a cone with the same thickness of the combustion chamber. The inclusion of the nozzle mass was intended to penalize large pressure ratios.

For the hydrogen peroxide case, a pressurization subsystem was necessary. The pressurization system mass was calculated based on the methodology presented by Sutton (2001). The gas (He) was assumed to be stored in a spherical carbon reinforced tank and was modeled as thin wall pressure vessel. The storage pressure and temperature of the gas were set at 400 bars and 300 K, respectively.

Recently, a model was proposed to calculate the oxidizer tank pressure history for nitrous oxide in the blowdown mode of operation (Whitmore and Chandler, 2010). The model was based on an entropy and mass balance using two-phase thermodynamics tables for dinitrogen monoxide. The model proposed by Whitmore and Chandler (2010) was validated in rapid depletion of oxidizer tank, typical of small sounding rockets operating without the help of a pressurization subsystem. In this study, however, the suggested operating time of the motor was long enough to allow consideration of equilibrium conditions (fluid saturation at some given temperature). Therefore, the pressure history was calculated from the energy balance applied to the fluid, assuming the tank as an adiabatic vessel. After a given time step, the actual mass in gas phase was corrected by a certain amount of nitrous oxide evaporated from the liquid phase. The enthalpy necessary to evaporate that mass determines the new temperature of the systems and as a consequence the latest tank pressure. In a future work we will make use of the model presented by Whitmore and Chandler (2010).

RESULTS AND DISCUSSION

The optimization code was then applied to help design the deboost engine based on the proposed configurations. The test cases are summarized in Table 3. For a given optimized design, the code determines the initial and final grain diameters, the solid fuel length, the chamber pressure, and the oxidizer mass flow rate. The results should be seen as a basis for preliminary Engineering design.

Table 3. Optimized motor configurations.

Test case	Type of oxidant	Scheme of oxidant injection	p_c [bar]	p_t [bar]
1	Hydrogen peroxide	Pressurized with He	≥ 10	$\geq 1.3\, p_c$
2	Hydrogen peroxide	Pressurized with He	≥ 30	$\geq 1.3\, p_c$
3	Nitrous oxide	Blowdown	≥ 10	$\geq 1.1\, p_c$

Test case 1

We start presenting the test case 1, based on hydrogen peroxide (90%) with 10-bar minimum combustion chamber pressure. This low-pressure level was set from a preliminary investigation, which showed that structural mass would penalize the overall mass of the system (main objective function). Low-pressure engine would give a poor specific impulse, but the mission (deboosting) requires a long time deceleration to improve reentry precision, therefore, a high-thrust level is not required and motor performance would not be a primary concern. The optimization process then brings the pressure of the system (~ 10.1 bars) closer to the lower acceptable limit, as Fig. 7 depicts. The dark symbols in the figure refer to a feasible engine, while the lighter ones showed unfeasible individuals, the ones that do not meet the design constraints (*Delta-V* and burning time constraints).

Figure 8 shows the convergence history for the grain external diameter. The convergence after 2,000 individuals approaches an external diameter of the order of 195 mm. At the same time, the suggested grain internal diameter approached 145 mm, as shown in Fig. 9. The burning thickness would be of the order of 25 mm. For a 55.34-second burning time, the expected mean regression rate would be lower than 0.5 mm/s, which could be attained with most of the solid fuels currently available.

Figure 10 presents the converged solution for the solid fuel length. As it can be seen, the system approaches a 488-mm value. The motor itself would claim a much longer room on account of the volume needed to accommodate the vaporization chamber, after oxidizer injection, the postcombustion chamber as well as the engine nozzle. Consequently, the motor would pose some difficulties in fitting the SARA reentry engine bay, if this type of limitation was put into consideration. In a different arrangement, in which nitrous oxide is the oxidizer, this parameter should not be a concern, as we will see later in this section.

Finally, as a design variable, the result for the initial

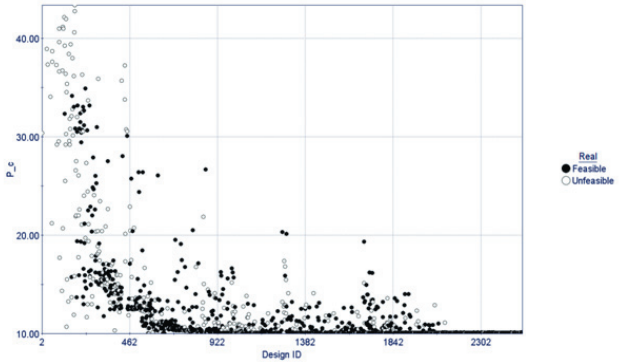

Figure 7. Convergence history of the combustion chamber pressure for case 1.

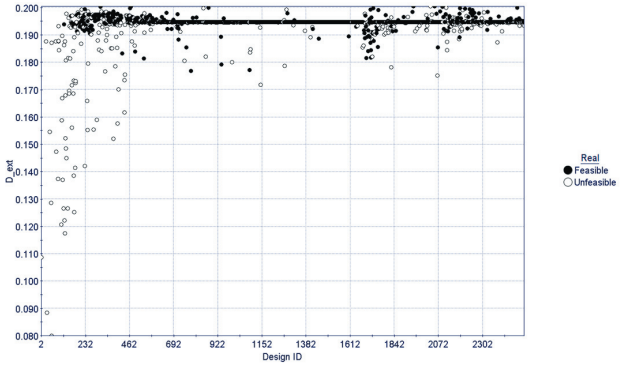

Figure 8.Convergence history of the solid fuel external diameter for case 1.

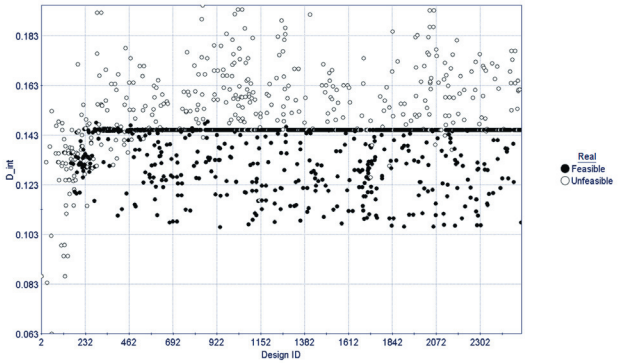

Figure 9. Convergence history of the solid fuel internal diameter for case 1.

oxidizer mass flow rate is presented in Fig. 11. Convergence approaches a value near to 260 g/s of the hydrogen peroxide. This can be easily attained with few pressure swirl atomizers placed at the oxidizer injection plate.

As for mission requirements and assumed constraints, Fig. 12 presents the convergence for spacecraft velocity reduction. Figure 13 shows the optimized motor operating time and Fig. 14, the overall mass of the system. The optimized overall mass of the engine was close to 22 kg. This engine would accomplish the mission with a velocity reduction of 235 m/s attained in near 55 seconds of burning time. This optimized engine mass is much lower than those calculated for liquid and solid propellant rockets (Villas Bôas *et al.*, 2000). These results imply that high-engine specific impulse could be considered of secondary relevancy for the reentry mission.

Figure 15 shows the influence of all the design variables on the engine constraints and mission requirements. A significant influence on the velocity reduction (*Delta-V*) comes from the initial oxidizer mass flow rate and the geometric parameters of the motor in the following order: solid fuel external diameter; solid fuel initial diameter, and solid fuel length. Thus, combustion chamber pressure claims a very weak influence on this mission requirement. The same trends can be observed for the thrust time (impulse): a rather strong influence on initial mass flow rate of oxidizer closely followed by the grain external diameter. Engine internal pressure, grain internal diameter and length somewhat share the remaining percentage of the influence. The total mass of the propulsive system is influenced, mainly, by the final geometric configuration (external and internal grain diameters) and mass flow rate of hydrogen peroxide. Combustion chamber pressure also causes weak influence on the overall mass of the propulsive

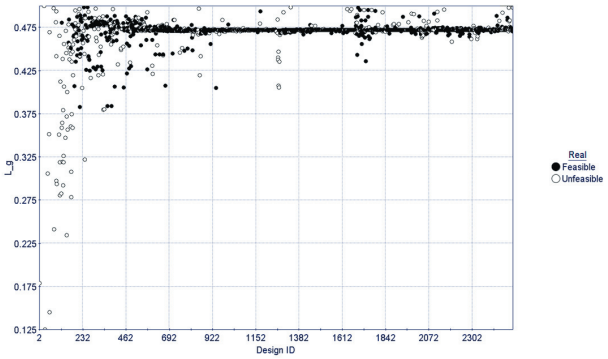

Figure 10. Convergence history of the solid fuel length for Case 1.

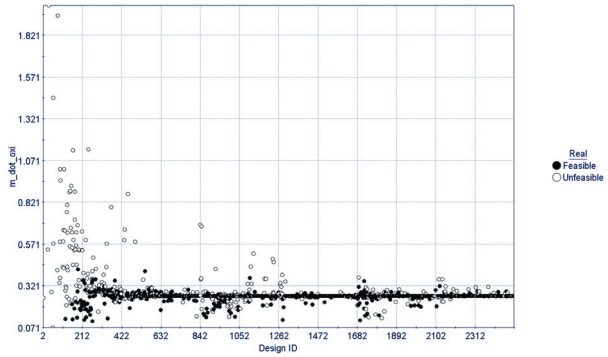

Figure 11. Convergence history of the initial mass flow rate of oxidizer for case 1.

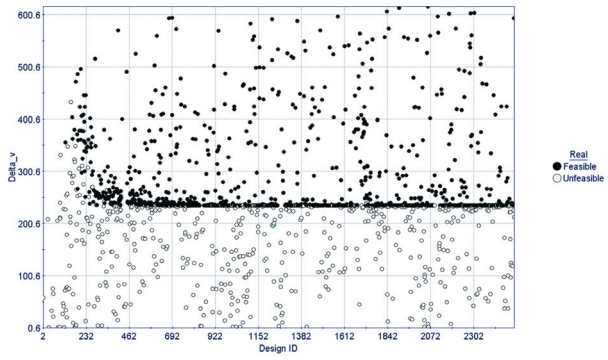

Figure 12. Convergence history of the velocity reduction for case 1.

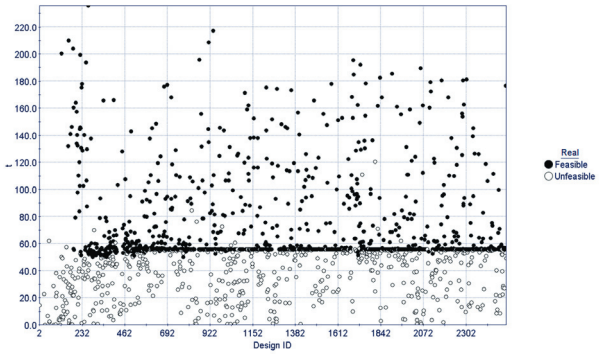

Figure 13. Convergence history of the engine burning time for case 1.

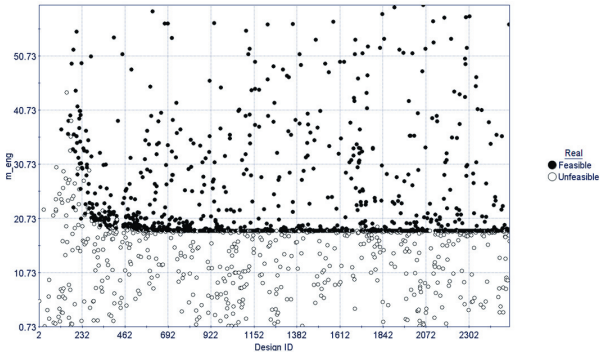

Figure 14. Convergence history of the engine overall mass (without correction) for case 1.

system. For the objective function (overall mass), combustion chamber pressure has a stronger influence on burning time and on velocity reduction. The operational envelope of the engine, as far as *OF* ratio is concerned, is largely influenced by the initial oxidizer mass flow rate and the grain external diameter. Conversely, the influence on the *OF* ratio is somehow shared among the remaining geometric parameters, in addition to the combustion chamber pressure. Finally, the influence of initial oxidizer mass flow rate along with the geometric parameters of the motor on the burning time show relatively comparable levels. The influence of the combustion chamber pressure on the solid fuel burning time can be considered negligible.

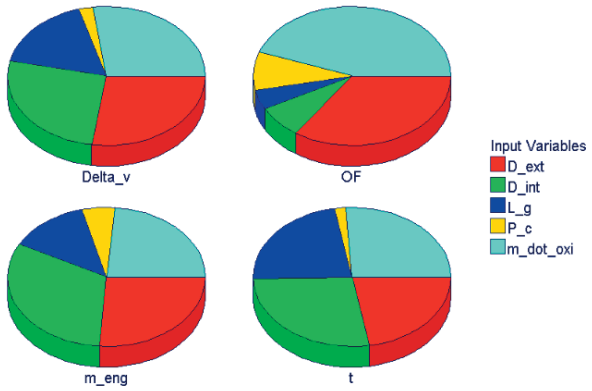

Figure 15. Influence of design variables on engine constraints and objective function for case 1.

Test case 2

In order to evaluate the engine design influence on the overall mass of the propulsive system, following mission requirements, a much higher combustion chamber pressure was imposed to the constraint of minimum operating pressure of the engine, based on hydrogen peroxide (90%). The optimized solution presented the following design variables and operating conditions of the engine:

- solid fuel external diameter – D_f = 172 mm;
- solid fuel length – L_g = 406 mm;
- internal port diameter – D_i = 123 mm;
- initial combustion chamber pressures – $p_{c,i} \leq 30$ bar; and
- initial oxidizer mass flow rate $\dot{m}_{oxi,0}$ = 260 g/s.

These figures are somehow close to those of test case 1, except the three-fold higher minimum operational combustion chamber pressure. As a consequence, a minor reduction in the burning time (1.2%) occurred, followed by a corresponding increase for the thrust engine level (~14%), a negligible reduction in the specific impulse (3.4%) and, at least, a two-fold increase in the expansion rate. Figure 16 shows the influence of the design variables on the engine constraints and on the mission requirements. As the combustion chamber pressure was increased, the influence of most design variables on the velocity reduction is of the same level, with the grain internal diameter showing the least share. The same trend holds to the engine burning time and overall mass. The combustion chamber pressure has also a considerable influence on the *OF* ratio, which was not observed for the optimized engine from the other cases. As a whole, this case resulted in an engine slightly heavier than that of case 1 configuration. Due to the fact that the only difference between the engine configuration, for cases 1 and 2, was the combustion chamber pressure, one could conclude that engine thrust, for the required mission, is not a primary design concern.

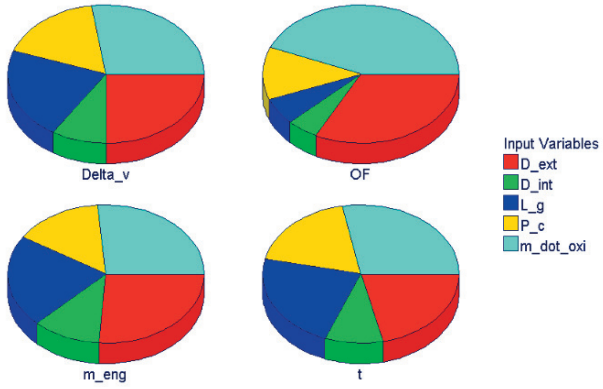

Figure 16. Influence of design variables on engine constraints and objective function for case 2.

Test case 3

Nitrous oxide has a high saturation pressure at ambient temperature (25°C). This self-pressurization characteristic of the oxidizer could be explored in this design assessment. Therefore, Test case 3 investigates a system configuration based on nitrous oxide and on solid paraffin propellants for the reentry engine of the SARA platform. Basically, the constraints for this case are the same as those imposed to the case 1 study, with the exception of a total absence of any pressurization subsystem. Oxidizer injection will take place on account of the N_2O self-pressurization inside the oxidizer tank by means of a series of pressure swirl atomizers. As oxidizer depletion takes place, a significant decay in the tank pressure is expected. This blowdown process was modeled based on the assumption of quasi-steady state for fluid exhaustion.

Figure 17 shows the influence of design parameters on mission requirements and the objective function. For this

configuration, the influence of pressure on overall mass of the engine, velocity reduction as well as burning time, is of the same order as those from the geometric parameters of the engine.

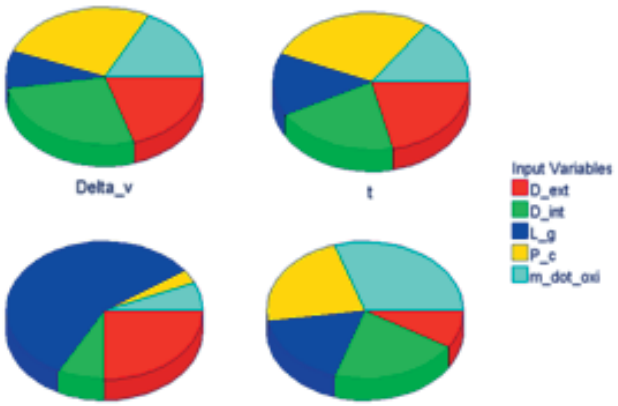

Figure 17. Influence of design variables on engine constraints and objective function for case 3.

Table 4. Deboost engine system for the three test cases.

Values	Test case 1	Test case 2	Test case 3
(m)	0.195	0.172	0.157
(m)	0.488	0.406	0.108
(m)	0.145	0.123	0.104
(bar)	10.086	30	10
(kg/s)	0.260	0.260	0.226
Delta-V (m/s)	235.13	235.0	235.0
t (s)	55.34	54.65	101.42
OF	7.80	7.836	8.312
Thrust coefficient	1.803	1.904	1.813
Specific impulse (s)	280.58	290.27	228.9
Expansion rate	12.76	30.69	12.69
Thrust (N)	733.5	835.06	494.13
Oxidant mass (kg)	14.46	14.18	18.21
Paraffin mass (kg)	1.829	1.78	2.032
Mass of the oxidant tank (kg)	0.449	1.317	3.822
Mass of the combustion chamber (kg)	0.695	1.360	0.140
Mass of the pressurization tank (kg)	0.658	2.120	–
Mass of the pressurization gas (kg)	0.261	0.842	–
Nozzle mass (kg)	0.077	0.162	0.080
Throat radius (m)	0.012	0.0068	0.0109
Nozzle exit radius (m)	0.042	0.0374	0.0390
Nozzle length (m)	0.157	0.1397	0.1455
System total mass (kg)	18.38	21.77	24.20
Corrected system mass (kg)	22.05	26.128	29.04

This configuration causes a strong difference on the mission execution and system design when compared to the use of hydrogen peroxide supported by a pressurization subsystem.

Table 4 presents the main parameters of this optimized configuration along with the results for cases 1 and 2. The important differences could be observed for solid fuel length, burning time, specific impulse, thrust, mass of oxidant, and total mass of the engine. The remaining parameters, as show in Table 5, are somewhat similar among any of the hydrogen peroxide configurations.

Table 5. Analysis of the proposed technologies for the SARA platform reentry system.

Parameter	LBP engine*	LMP engine*	SP engine*	HP engine
Mass	High – 47 kg	Middle – 40 kg	Low – 35.1 kg	Low – 20 kg
Technical challenges	High	High	Low	Low
Development status	Low	Middle	High	Middle
Production cost	High	Middle	Low	Low
Operating precision	High	High	Low	High
Handling, safety, and toxicity	High care	High care	Middle care	Low care

LBP: liquid bipropellant; LMP: liquid monopropellant; SP: solid propellant; HP: hybrid propellant. *Villas Bôas *et al.* (2000).

Table 5 summarizes the explored technologies that may execute the reentry maneuver of the SARA platform. Relevant parameters were investigated and compared among different motor configurations, three from a previous study (Villas Bôas *et al.*, 2000) and one selected from this work. The optimized hybrid propellant rocket configuration seems to be a very attractive technological solution for the reentry system, on account of the inherent aforementioned advantages over solid and liquid counterparts and, more importantly, the resulted lower mass of the engine.

Figure 18 shows a hybrid rocket engine operating in a test stand. The engine makes use of nitrous oxide and paraffin as the propellants. Following the large external diameter, the burning time of such motor would match that calculated for case 3, for an equivalent thrust. Some level of thrust variation was accomplished in this test campaign, suggesting a much less effort on developing such solution for the SARA platform.

Figure 18. A paraffin/N_2O hybrid rocket firing test at the University of Brasília.

CONCLUSIONS

Optimized hybrid propellant rocket engines, based on three different configurations, were proposed as main components of the deboost system of the Brazilian SARA platform. All three configurations resulted in engines lighter than the liquid and solid motors previously studied. The inherent advantages of hybrid propulsion system, over more traditional counterparts, should be taking into consideration following this assessment. Hybrid rocket technology would increase system reliability for the required mission, considering that the propulsive components are readily available in the Brazilian space industry at very competitive cost. The optimization process discussed in this work can be considered an essential tool for the preliminary phase design of hybrid rocket propulsive systems for a given application.

ACKNOWLEDGEMENTS

The authors thank the Agência Espacial Brasileira (Programa Uniespaço) and Conselho Nacional de Desenvolvimento Científico e Tecnológico (CNPq) for their support.

REFERENCES

Akhtar, S.and Lin-shu, H., 2007, *"*Optimization and Sizing for Propulsion System of Liquid Rocket Using Genetic Algorithm*"*, Chinese Journal of Aeronautics, Vol. 20, No. 1, pp. 40-46.

Almeida, L. A. R. and Santos, L. M. C., 2005, "Design, fabrication and launch of a hybrid rocket with paraffin and N_2O propellants" (In Portuguese), Graduation Project, Mechanical Engineering Department, University of Brasília, Brasília, D. F., Brazil, 83p.

Altman, D. and Holzman, A., 2007, "Overview and History of Hybrid Rocket Propulsion." In Chiaverini, M.J., Kuo, K.K. (ed.), Fundamentals of Hybrid Rocket Combustion and Propulsion, American Institute of Aeronautics and Astronautics, Inc., Reston, Virginia, Vol. 218, Chapter 1, pp. 01-36.

Anderson, M.B., 2002, "Genetic Algorithms In Aerospace Design: Substantial Progress Tremendous Potential." Paper presented at the RTO AVT Course on "Intelligent Systems for Aeronautics", held in Rhode-Saint-Genèse, Belgium, 13-17 May 2002, and published in RTO-EN-022.

Bertoldi, A. E. M., 2007, "Experimental investigation of the burning of paraffin and nitrous-oxide in hybrid rocket engines (In Portuguese), Master Thesis, Mechanical Engineering Department, University of Brasília, Brasília, D. F., Brazil, 115p.

Brown, T. R. and Lydon, M. C., 2005, "Testing of Paraffin-Based Hybrid Rocket Fuel Using Hydrogen Peroxide Oxidizer", AIAA Region 5 Student Conference, Wichita, USA.

Campbell, J.*et al.*, 2008, "Handling considerations of nitrous oxide in hybrid rocket motor testing", Proceedings of AIAA 2008-4830 44th AIAA/ASME/SAE/ASEE Joint Propulsion Conference & Exhibit, Poway, California, pp. 3177-3183.

Casalino, L. and Pastrone, D., 2005, "Oxidizer Control and Optimal Design of Hybrid Rockets for Small Satellites." Journal of Propulsion and Power, Vol. 21, pp. 230-238.

Contaifer, R. A., 2006, "Qualification and flight tests of the SD-1 sounding rocket" (In Portuguese), Graduation Project, Mechanical Engineering Department, University of Brasília, Brasília, D. F., Brazil, 75p.

Costa, F.S. and Vieira, R., 2010, "Preliminary Analysis of Hybrid Rockets for Launching Nanosats into LEO*"*, ABCM, Vol. 32, No. 4, pp. 502-509.

DaLin, R. *et al.*, 2012, "Design and Optimization of Variable Thrust Hybrid Rocket Motors for Sounding Rockets, Science China", Technological Sciences, Vol. 55, No. 1, pp. 125-135.

Davydenko, N. A. *et al.*, 2007, "Hybrid rocket engines – the benefits and prospects", Aerospace Science and Technology, Vol. 11, pp. 55-60.

Greatrix, D.R., 2009, "Regression rate estimation for standard-flow hybrid rocket engines", Aerospace Science and Technology, Vol. 13, pp. 358-363.

Karabeyoglu, M. A. *et al.*, 2004, "Scale-up Tests of High Regression Rate Paraffin-BasedHybrid Rocket Fuels.", Journal of Propulsion and Power, Vol. 20, No. 6, pp. 1037-1045.

Karabeyoglu, M. A., 2008, "Hybrid propulsion for future space launch", 50th Anniversary Symposium and Celebration, University of Stanford Aero/Astro Symposium, Palo Alto, California.

Koldaev, V. and Moraes, P. Jr., 1997, "Design of a recovery system for small orbital payloads", Proceedings of the 14th Brazilian Congress of Mechanical Engineering, Bauru, São Paulo, Brazil.

Kwon, S. T. *et al.*, 2003, "Optimal design of hybrid motor for the first stage of air launch vehicle", Proceedings of the 39th AIAA/ASME/SAE/ASEE Joint Propulsion Conference and Exhibit, Huntsville, Alabama.

Oiknine, C., 2006, "New perspectives for hybrid propulsion", Proceedings of the AIAA paper 2006-4674, 42nd AIAA/ASME/SAE/ASEE Joint Propulsion Conference and Exhibit, Sacrameno, California.

Rhee, I.*et al.*, 2008, "Optimal Design for Hybrid Rocket engine for Air Launch Vehicle", Journal of Mechanical Science and Technology, Vol. 22, pp. 1576-1585.

Santos, L. M., C. *et al.*, 2006, "Experimental investigation of a paraffin based hybrid rocket*"*, Thermal Engineering, Vol. 5, No. 1, pp. 08-12.

Sasaki, D. and Obayashi, S., 2005, *"Efficient Search for Trade-offs by Adaptive Range Multi-Objective Genetic Algorithms", J*ournal of Aerospace, Computing, Information and Communication, Vol. 2, pp. 44-64.

Sutton, G. P., 2001, "Rocket propulsion elements: an introduction to the engineering of rockets", 7th edition, New York, USA, John Wiley & Sons,

Viegas, F. L. and Salemi, L. C., 2000, "Design and assembling of a static test bench for hybrid rocket engines" (In Portuguese), Graduation Project, Mechanical Engineering Department, University of Brasília, Brasília, D.F.

Villas Bôas, D. J. F.*et al.*, 2000, "Studies on the characteristics of de-boost motors for a small recoverable orbital platform", Proceedings of the National Congress of Mechanical Engineering, Natal, R.N., Brazil.

Whitmore, S. A. and Chandler, S. N., 2010, "Engineering Model for Self-Pressurizing Saturated-N2O-Propellant Feed Systems", Journal of propulsion and Power, Vol. 26, No. 4, pp. 706-714.